NASA TECHNICAL MEMORANDUM

NASA TM X-52779

NASA TM X-52779

EVALUATION OF ELECTRON-BEAM WELDED HOLLOW BALLS FOR HIGH-SPEED BALL BEARINGS

by Harold H. Coe, Richard J. Parker, and Herbert W. Scibbe
Lewis Research Center
Cleveland, Ohio

TECHNICAL PAPER proposed for presentation at Spring Lubrication Symposium sponsored by the American Society of Mechanical Engineers
Detroit, Michigan, May 25-27, 1970

EVALUATION OF ELECTRON-BEAM WELDED HOLLOW BALLS FOR HIGH-SPEED BALL BEARINGS

by Harold H. Coe, Richard J. Parker, and Herbert W. Scibbe

Lewis Research Center
Cleveland, Ohio

TECHNICAL PAPER proposed for presentation at

Spring Lubrication Symposium
sponsored by the American Society of Mechanical Engineers
Detroit, Michigan, May 25-27, 1970

NATIONAL AERONAUTICS AND SPACE ADMINISTRATION

EVALUATION OF ELECTRON-BEAM WELDED HOLLOW BALLS FOR HIGH-SPEED BALL BEARINGS

by Harold H. Coe, Richard J. Parker
and Herbert W. Scibbe

E-5442

ABSTRACT

An experimental investigation was performed with two series (115 and 215) of 75 mm bore ball bearings using hollow balls as the rolling elements. The bearings were tested at 500 and 1000 pounds thrust loads at shaft speeds up to 24000 rpm. The 115 series bearings with 1/2-inch SAE 52100 steel balls showed very little difference in torque, outer-race temperature, or rolling-element fatigue life when compared to similar data for a solid ball bearing. The 215 series bearings with 11/16-inch AISI M-50 steel balls showed only slight differences in torque and outer-race temperature, but a very significant decrease in rolling-element fatigue life compared to a solid ball bearing. The balls failed in flexure fatigue, due to a stress concentration in the weld area.

- - - - -

Proposed paper for the ASME Spring Lubrication Symposium, Detroit, Michigan May 25-27, 1970.

EVALUATION OF ELECTRON-BEAM WELDED HOLLOW BALLS FOR HIGH-SPEED BALL BEARINGS

by Harold H. Coe, Richard J. Parker
and Herbert W. Scibbe

INTRODUCTION

Recent developments in gas turbine engines--such as advanced compressor design, high temperature materials, and improved power output--have resulted in larger shaft diameters and higher main shaft bearing speeds [1].[1] Bearings in current production aircraft turbine engines operate in the range from 1.5 to 2 million DN (bearing bore in mm times shaft speed in rpm). Engine designers anticipate that, during the next decade, turbine bearing DN values will have to increase to the range of 2.5 to 3 million. It is speculated that after 1980, turbine engine developments may require bearing DN values as high as 4 million.

When ball bearings are operated at DN values above 1.5 million, high centrifugal forces are produced by the balls. These high centrifugal forces result in high Hertz stresses at the outer-race ball contacts and thus seriously affect bearing life [2].

Operation at higher DN values also results in higher heat generation. Excessive heat generation can result from ball skidding [3] or ball spinning [4]. The heat generated within the bearing must be removed, or a loss in operating clearance will occur and the bearing will fail. Refinements in bearing internal geometry--such as using smaller diameter balls, larger diametral clearances, or more open race curvatures--can effectively reduce

- - - - - -

[1]Numbers in brackets designate references at end of paper.

heat generation and/or centrifugal force. The degree of improvement is limited, however, since the geometrical changes that reduce heat generation will generally reduce fatigue life [5].

Another possible solution to problems caused by ball centrifugal force or excessive heat generation is the use of hollow balls in the bearing. Obviously, removal of a large percentage of the mass from the ball will reduce the centrifugal force. In [6], an analysis was made that predicted some advantages of hollow balls over solid balls in a high speed thrust bearing. The analysis showed that, at a 3 million DN value, using hollow balls with an outer-to-inner-diameter ratio of 1.25 (51 percent weight reduction), reduced the ball spin-to-roll ratio as much as 25 percent. (Ball spin-to-roll ratio is a measure of the total rolling contact torque. The lower this ratio, the lower will be the bearing ball-spin torque and thus the heat generation).

The feasibility of fabricating hollow balls by electron-beam welding of two hemispherically formed shells has been adequately demonstrated [7] and [8]. In order to evaluate the performance of hollow balls in rolling-element fatigue tests and full-scale bearing tests the research reported herein was undertaken. These data and analysis are also reported in [9] and [10].

The objectives of the present investigation were (1) to determine experimentally the operating characteristics of a full-scale bearing using hollow balls as the rolling elements, (2) to compare the torque and outer-race temperature data of the bearing with the hollow balls to data of a similar bearing with solid balls and (3) to determine the rolling-element fatigue lives of the hollow balls relative to the lives of solid balls.

Tests were conducted with two series (115 and 215 series) of 75 mm-bore deep-groove ball bearings using both hollow and solid balls. The bearings were operated at 500 and 1000 pound thrust loads and at speeds up to 24000 rpm (1.8×10^6 DN) using air-oil-mist lubrication. The hollow balls for the 115 series bearings were 1/2-inch diameter with a 0.100-inch wall thickness (a weight reduction of 21.7 percent from that of the solid balls). The hollow balls for the 215 series bearings were 11/16-inch diameter with a 0.060-inch wall thickness (a weight reduction of 56.5 percent from that of the solid balls).

Rolling-element fatigue tests were run in the five-ball fatigue tester with both the 1/2-inch and the 11/16-inch diameter hollow balls as upper balls. The results were compared with solid balls tested under identical or adjusted conditions.

APPARATUS

Bearing Test Rig

A cutaway view of the bearing test apparatus is shown in figure 1. A variable-speed, direct current motor drives the test bearing shaft through a gear speed increaser. The ratio of the test shaft speed to the motor shaft speed was 14 to 1.

The test shaft was supported and cantilevered at the driven end by two oil-jet lubricated ball bearings. The test bearing was thrust loaded by a pneumatic cylinder through an externally pressurized gas thrust bearing.

Bearing torque was measured with an unbonded strain gage force transducer, connected to the periphery of the test bearing housing, as shown in figure 1. This torque was recorded continuously by a millivolt potentiometer. The estimated accuracy of the data recording system was $\pm$0.05 lb-in.

Bearing outer-race temperature was measured with two iron-constantan thermocouples located as shown in figure 1. The estimated accuracy of the temperature measuring system was about $\pm$2° F.

The test bearing was lubricated by an air-oil mist. The oil flow rates ranged from 0.01 to 0.07 pounds per minute. The lubricant used in this investigation was a super-refined naphthenic mineral oil with a viscosity of 75 centistokes at 100° F.

Five-Ball Fatigue Tester

The NASA five-ball fatigue tester was used for the hollow ball fatigue tests. The apparatus, shown in figure 2, is described in detail in [11]. This fatigue tester consists essentially of an upper test ball pyramided upon four lower support balls that are positioned by a separator and are free to rotate in an angular contact raceway. Load is applied to the upper test ball through a vertical shaft that drives the ball assembly.

Test Bearings and Hollow Balls

The test bearing specifications are listed in table 1. Two series (115 and 215) of 75 mm bore, deep-groove ball bearings were used with both solid and hollow balls. The 115 series bearings used 1/2-inch diameter balls and the 215 series used 11/16-inch diameter balls. A photograph of the test bearings is shown in figure 3.

The 1/2-inch diameter hollow balls had a wall thickness of 0.100 inches. The ratio of the outside-to-inside diameter (OD/ID) was 1.67 and the weight reduction was 21.7 percent from that of a solid ball. The hollow 1/2-inch balls were made from SAE 52100 consumable electrode, vacuum melt (CVM), steel with a nominal hardness of Rockwell C 65.

The 11/16-inch diameter hollow balls had a wall thickness of 0.060 inches. This is an OD/ID ratio of 1.21 with a weight reduction of 56.5 percent from that of a solid ball. The 11/16-inch hollow balls were fabricated from AISI M-50 CVM steel with a nominal Rockwell C hardness of 63.5.

A chemical analysis of the materials from which both size hollow balls were made is given in table 2. The heat treatment schedule for both materials is given in table 3.

PROCEDURE

Bearing Tests

Each test bearing was run-in for one hour with a 250 pound thrust load, a shaft speed of 6000 rpm, and an air-oil mist flow rate of about 0.010 pounds per minute. After run-in, the thrust load was set at 500 pounds, the air-oil mist flow rate was increased to 0.037 pounds per minute and the shaft speed was increased to 10 000 rpm. Each bearing was operated at this initial condition until temperature equilibrium was achieved. Equilibrium was assumed for each data point when the bearing outer-race temperature reading had not changed more than 1° F over a ten minute interval.

After the initial data point was taken, the shaft speed was taken, the shaft speed was increased to 2000 rpm increments while the load was maintained constant. The lubricant flow rate was increased with the shaft

speed as shown in table 4. The calculated minimum oil-flow rates shown in table 4 were determined by the technique described in [12]. Outer-race temperature and bearing torque were recorded for each shaft speed. Data points were taken until either the bearing lost clearance, or outer-race temperature equilibrium could not be attained. For the 1000 pound thrust load tests, the thrust load was increased after the initial data point at 10 000 rpm, and the procedure repeated.

Fatigue Tests

The fatigue tests were conducted in the five ball fatigue tester running at 10 600 rpm. The outer race temperature stabilized at 145 to 150° F with no heat added. The lubricant was the same super-refined naphthenic mineral oil used in the bearing tests. The tests were run continuously until failure of either an upper test ball or a lower ball occurred or until a preset cutoff time.

One-half-inch- diameter hollow balls. Both hollow and solid 1/2-inch diameter balls from one heat of SAE 52100 CVM steel were tested at a maximum Hertz stress of 800 000 psi and a contact angle of 20° (indicated by β in figure 2 (b)). Lower balls were 1/2-inch diameter SAE 52100 balls with a nominal Rockwell C hardness of 63.

Eleven-sixteenths-inch diameter hollow balls. The 11/16-inch diameter AISI M-50 CVM hollow balls were run at a maximum Hertz stress of 700 000 psi. Lower balls were 1/2-inch diameter solid AISI M-50 with a nominal Rockwell C hardness of 64. The contact angle β of this configuration using a modified raceway was 34.5° (figure 2 (b)).

Post-Test Inspection

After test, the bearings were disassembled, cleaned and inspected for damage.

After the fatigue tests, the hollow balls were cleaned and examined. The balls were electropolished to determine the location of the weld, the orientation of the weld relative to the ball track, and the proximity of the fatigue spall to the weld area.

Some balls were sectioned through and parallel to the track. The sections were polished and photomicrographs were taken.

RESULTS AND DISCUSSION

Bearing Tests

Two series (115 and 215) of 75 mm bore ball bearings were tested with solid and hollow rolling elements to determine their operating characteristics. The results of tests with the 115 size bearings are shown in figure 5. There is very little difference in either the outer-race temperature (figure 4 (a)) or the total bearing torque (figure 4 (b)) between the bearing with the solid balls and the bearing with the hollow balls over the range of shaft speeds investigated.

The results of tests with the 215 size bearings are shown in figure 5. The curves of outer-race temperature (figure 5(a)) and bearing torque (figure 5 (b)) against speed show that the hollow ball bearings had slightly lower values than the solid ball bearing for the range of shaft speeds investigated.

Bearing Post-Test Inspection

Visual inspection of the 115 series bearings showed that the balls, races and retainers were in very good conditions, with no apparent wear or other damage.

Inspection of the 215 series bearings, however, showed extensive damage to the hollow balls. A photograph of several typically damaged balls is shown in figure 6. The ball damage ranged from spalling (figure 6 (a)) to complete fracture (figure 6 (b)). The spalls were all on the running track. The ball in figure 6 (b) fractured into two halves at the weld. The weld was perpendicular to the track and a spall was right at the weld.

One ball from bearing 215-1-H had 14 spalls around its circumference; upon sectioning this ball, it was determined that the ball track was completely on top of the weld, as shown in figure 7. Further examination of this ball showed many cracks on the internal surface, across the weld, as shown in figure 8. This ball was then sectioned parallel to and through the track and the specimen polished. A composite of several photomicrographs, shown in figure 9, reveals a pattern of cracks from the inside of the ball to the outside surface spalls.

Other balls that were damaged were electropolished to determine the orientation of the weld relative to the running track. All of these tracks were at angles from 45 to 90° to the weld. Every ball that was sectioned parallel to and through the track revealed cracks between the weld area and the outside surface, an example of which is shown in figure 10.

It was not apparent from these photographs whether the cracks were forming at the outside surface and propagating inward, or forming at the inside surface and propagating outward through the wall, resulting in a surface spall. However, several balls that did not show surface distress were sectioned parallel to and through the ball track. In each of these balls, cracks were revealed that apparently had originated at the inside surface in the weld area, as shown in figure 11.

Several observations on the integrity of the weld were made. Microhardness measurements made on a sectioned ball in the weld zone and in the parent material showed a variation in Rockwell C hardness of less than 2 points. A slight difference in microstructure was also observed, but this difference was not considered significant.

The electron beam weld appeared to be of good quality and proper technique. The bead on the inside surface of the balls, however, was variable in thickness around the circumference. There was considerable spatter of material on the inside surface of the ball. In some sectioned specimens, the wall thickness was slightly less adjacent to the weld than in the remainder of the wall. This possibly resulted from misalignment of the two hemispherical shells in the welding fixture.

Two hollow balls that had not been run were examined by X-ray techniques and no cracks were observed. Three hollow balls that had been run in a bearing but had no apparent surface defects were then examined by X-ray, and cracks were observed in all three.

From the above examination, it was concluded that the hollow balls from the 215 series bearings had probably failed in flexure due to a stress concentration in the region of the weld. This stress concentration appeared in nearly all cases to be at the notch formed at the edge of the weld bead.

Fatigue Tests

One-half-inch diameter hollow balls. Groups of 1/2-inch diameter hollow and solid balls fabricated from one heat of SAE 52100 CVM steel were tested as upper ball specimens in the five-ball fatigue tester. The nominal wall thickness of these hollow balls was 0.100 inch (21.7 percent weight reduction). The results of the fatigue tests are shown in figure 12. This figure is a plot of the log-log of the reciprocal of the probability of survival as a function of the log of the stress cycles to failure (Weibull coordinates). For convenience, the ordinate is graduated in statistical percent of specimens failed. The 10-percent life for the solid balls was 93 million stress cycles as opposed to 60 million stress cycles for the hollow balls. This difference in fatigue life was not considered sufficiently significant to state that the welded hollow balls were inferior to the conventional solid balls.

Examination of the 27 hollow balls tested revealed that 10 had failed by what appeared to be classical subsurface fatigue. Of these 10 failures only one occurred at or near the weld.

The probability of a failure occurring in the weld, if the weld area is assumed to be of equal fatigue strength to the area outside the weld, is the ratio of the length of the running track in the weld to the total track length on the ball. The track length in the weld for each hollow ball,

in which the running track crossed the weld, was measured. The probability of a weld failure was determined to be approximately 6.5 percent for the group of hollow balls. One failure, out of a total of ten, occurring in the weld would therefore not be unexpected.

Examination of the microstructure of the weld indicates very little difference between it and that of the parent material. A hardness variation of less than 1 point Rockwell C between the weld and parent material indicated very good control during the manufacturing process.

It is concluded that for these hollow balls, the weld zone material is not significantly weaker in rolling-element fatigue than the solid parent material.

Eleven-sixteenths-inch diameter hollow balls. A group of seven 11/16-inch diameter AISI M-50 CVM steel hollow balls were also tested as upper balls in the five-ball fatigue tester. The wall thickness was 0.060 inch (weight reduction of 56.5 percent). The results of these were plotted on Weibull coordinates as shown in figure 13. For comparison, data for AISI M-50 steel solid balls from [13] was adjusted for similarity of test conditions and plotted in figure 13. The fatigue lives are obviously much lower for the hollow balls than for the solid balls.

The seven hollow balls were electropolished to determine the orientation of the weld. On each of six failed balls, the running track crossed the weld. The fatigue spall on five of these six balls was adjacent to or directly on the weld. The spall on the other ball was clearly away from the weld area. The running track on the seventh ball did not cross the weld. This ball had no fatigue spall after 300 hours (530 million stress cycles) running time.

Four of the failed balls with the spall adjacent to the weld were sectioned parallel to and through the running track. In each ball, a crack was found that passed through the weld area and connected the outside surface spall to the inside surface. A typical crack is shown in figure 14.

From the width, shape, and pattern of these cracks, it was concluded that they initiated at the inner surface of the ball and propagated to the outer surface, resulting in a spall that resembled those of classical subsurface rolling-element fatigue. It was also concluded that these hollow balls from the fatigue tests had probably failed in flexure due to a stress concentration in the region of the weld, in the same manner as the balls in the 215 series bearings. Again, the stress concentration appeared to be at the notch formed at the edge of the weld.

The ball with the spall away from the weld area was also sectioned through the spall parallel to the running track. No cracks could be seen connecting the spall and the inner surface of the ball. This failure was apparently not a result of flexure of the wall, and most probably was classical subsurface fatigue.

CONCLUDING REMARKS

The 1/2-inch diameter, SAE 52100 steel hollow balls, with an outside-to-inside diameter ratio (OD/ID) of 1.67 compared satisfactorily with solid balls in fatigue tests. However, the 11/16-inch diameter, M-50 steel hollow balls with an OD/ID ratio of 1.21 did not compare very well with solid balls in fatigue tests. The fact that the balls were of different material and

size should not have made any significant difference in the fatigue comparisons. It is probable that the OD/ID ratio of 1.21 results in a wall that is merely too thin for use as a bearing ball.

The 115 series hollow ball bearings did not have any ball failures, but showed no marked improvement over the solid ball bearings over the range of shaft speeds tested. The 215 series hollow ball bearings did have ball failures, but otherwise showed some improvement in operation over the solid ball bearings. However, a combination of the air-oil-mist lubrication system and the temperature limitation of the SAE 52100 steel (hot hardness) limited the testing of the 115 series bearings to moderate speeds. This does not preclude the possibility that some improvement in operation would be noted if the bearing could have been operated at higher shaft speeds. The use of hollow balls in bearings could still be advantageous at higher DN values if the wall thickness of the balls is such that the flexure problem is minimized.

A number of problems exist with hollow balls for use in bearings that are inherent in the manufacture of the ball. Two significant problems are: (1) difficulty in maintaining uniform wall thickness and (2) controlling the weld penetration around the periphery of the ball. Unless these problems are overcome hollow balls will have an unbalance and/or a slightly different stiffness at the weld. Under dynamic conditions, these factors could adversely affect the life of the ball.

SUMMARY OF RESULTS

An experimental investigation was conducted to determine the operating characteristics of full-size bearings using hollow balls as the rolling elements. Two series of 75 mm bore deep-groove ball bearings were operated at shaft speeds up to 24 000 rpm (1.8×10^6 DN) with thrust loads of 500 and 1000 pounds. The 115 series bearings used 1/2-inch diameter balls with a 0.100-inch wall thickness and the 215 series bearings used 11/16-inch diameter balls with a 0.060-inch wall thickness. The torque and outer-race temperature data of the bearings with the hollow balls were compared to data of similar bearings with solid balls. The following results were obtained:

1. The 11/16-inch diameter hollow balls failed apparently by flexure fatigue. Cracks initiated at the inner diameter at a stress concentration in the weld area and propagated through the wall, terminating in a spall on the outer surface.

2. Rolling-element fatigue life of the 11/16-inch diameter hollow balls, determined at 700,000 psi maximum Hertz stress in a five-ball fatigue tester was significantly less than lives predicted from previously run AISI M-50 solid steel balls. The hollow balls from the fatigue tests appeared to have failed in flexure, like those balls from the 215 series bearings.

3. The total bearing torques and outer-race temperatures of the 115 series hollow ball bearings operating at speeds up to 18 000 rpm (1.35×10^6 DN) were not significantly different from those of the 115 series solid ball bearings.

4. The bearing torque and outer-race temperature of the 215 series hollow ball bearings were slightly lower than the corresponding values for the 215 series solid ball bearings over the range of test conditions investigated.

5. Rolling-element fatigue life of the 1/2-inch diameter hollow balls was not significantly less than that obtained with solid balls. Only one of the ten fatigue spalls on the hollow balls occurred on a weld.

REFERENCES

1. P. F. Brown, "Discussion of Paper Previously Published in ASLE Trans. (ref. 6 below)," ASLE Transactions, vol. 12, no. 3, July 1969, pp. 204-205.

2. A. B. Jones, "The Life of High-Speed Ball Bearings," ASME Transactions, vol. 74, no. 5, July 1952, pp. 695-703.

3. P. S. Kliman, "High Speed Ball Bearings - Limitation and Thrust Requirements," Lubrication Engineering, vol. 20, no. 4, April 1964, pp. 151-154.

4. E. E. Bisson and W. J. Anderson, "Advanced Bearing Technology," NASA SP-38, 1964, pp. 159-164, 311-321.

5. J. T. Mayer and T. C. Litzler, "An Approximate Determination of the Effects of Geometry on Ball Bearing Torque and Fatigue Life," NASA TN D-2792, 1965.

6. T. A. Harris, "On the Effectiveness of Hollow Balls in High-Speed Thrust Bearings," ASLE Transactions, vol. 11, no. 4, October 1968, pp. 290-294.

7. P. R. Eklund, "Test on a Three-Inch Hollow Ball," Research and Technology Briefs, Air Force Flight Dynamics Laboratory, vol. IV, no. 10, November 1966.

8. H. Hanau, et al., New Concepts in Bearing Designs and Applications, Industrial Tectonics, Inc., Compton, Calif., 1965, pp. 20-23.

9. H. W. Scibbe, R. J. Parker, and E. V. Zaretsky, "Rolling-Element Fatigue Life of SAE 52100 Steel Hollow Balls," NASA TN D-3832, 1967.

10. H. H. Coe, H. W. Scibbe, and R. J. Parker, "Performance of 75 mm-Bore Bearing to 1.8 Million DN Using Electron-Beam Welded Hollow Balls," proposed NASA Technical Note.

11. T. L. Carter, E. V. Zaretsky, and W. J. Anderson, "Effect of Hardness and Other Mechanical Properties on Rolling-Element Fatigue Life of Four High Temperature Bearing Steels," NASA TN D-270, 1960.

12. Z. N. Nemeth and W. J. Anderson, "Effect of Speed, Load, and Temperature on Minimum-Oil-Flow Requirements of 30- and 75-Millimeter-Bore Ball Bearings," NASA TN D-2908, 1965.

13. R. J. Parker and E. V. Zaretsky, "Rolling Element Fatigue Life of Ausformed M-50 Steel Balls," NASA TN D-4954, 1968.

TABLE I. - BEARING SPECIFICATIONS

Bearing	Type Series	Deep groove 115	Deep groove 115	Deep groove 215	Deep groove 215
	Bore, mm Outer diameter, mm	75 115	75 115	75 130	75 130
	Grade Radial clearance, in.	ABEC-5 0.0027	ABEC-5 0.0027	ABEC-5 0.0020	ABEC-5 0.0020
Ball	Number per bearing Outside diameter, in.	14 0.500	14 0.500	11 0.6875	11 0.6875
	Wall thickness, in. Material	Solid SAE 52100 CEVM	0.10 SAE 52100 CEVM	Solid AISI M-2 CEVM	0.060 AISI M-50 CEVM
Races	Curvature, inner/outer Material	0.54/0.54 SAE 52100 CEVM	0.54/0.54 SAE 52100 CEVM	0.53/0.53 AISI M-2 CEVM	0.53/0.53 AISI M-2 CEVM
Retainer	Design Locating surface	One-piece machined Inner race	One-piece machined Inner race	Two-piece machined, riveted Outer race	Two-piece machined, riveted Outer race
	Material	Silver-plated bronze	Silver-plated bronze	Annealed AISI M-2	Annealed AISI M-2

TABLE II. - CHEMICAL ANALYSIS OF HOLLOW BALL MATERIALS

Material	Analysis, percent by weight											
	C	Si	Mn	S	P	W	Cr	V	Mo	Co	Ni	Cu
SAE 52100 (CVM)	1.03	0.26	0.34	0.005	0.010	----	1.53	----	0.03	----	0.05	0.08
AISI M-50 (CVM)	.79	.22	.23	.004	.008	0.02	4.05	1.04	4.20	0.02	.04	.02

TABLE III. - HOLLOW BALL MATERIAL HEAT TREATMENT

[Melting process, consumable electrode vacuum melt]

Material	Anneal after EB welding	Austenitize, °F	Quench, °F	First temper, °F	Second temper, °F	Third temper, °F	Nominal hardness, Rockwell C
SAE 52100	(1) Heat to 1475° F (2) Hold for 7 hr[a] (3) Furnace cool to 300° F at 20° F/hr (4) Aircool to room temperature	1550 for 12 min	Oil to room temperature	1020 for 180 min	1045 for 120 min[c]	1050 for 120 min	65
AISI M-50	(1) Heat to 1500° F (2) Hold for 2 hr[b] (3) Furnace cool to 1050° at 50° F/hr (4) Aircool to room temperature	2065 for 6 min	Molten salt to 1050° F aircool to room temperature	275 for 60 min	---------	--------	63.5

[a]In spent cast iron chips.
[b]In stainless steel bag.
[c]Subzero cool to -150° F for 2 hr.

TABLE IV. - LUBRICANT FLOW RATES

Shaft speed, rpm	Thrust load = 500 lb		Thrust load = 1000 lb	
	Calculated minimum flow rate, lb/min (a)	Oil flow rate in test, lb/min (b)	Calculated minimum flow rate, lb/min (a)	Oil flow rate in test, lb/min (b)
10 000	0.0004	0.037	0.0014	0.037
12 000	.0010	.037	.0035	.037
14 000	.0023	.037	.0081	.037
16 000	.0046	.046	.0165	.062
18 000	.0086	.062	.031	.073
20 000	.0149	.073	.054	----
22 000	.024	.073	.087	----
24 000	.039	.073	.139	----
26 000	.059	----	.208	----
28 000	.087	----	.305	----
30 000	.126	----	.450	----

[a]Calculated from ref. 12 using T = 400° F for 75 mm bore bearing.

[b]Introduced to bearing as an air-oil mist.

E-5442

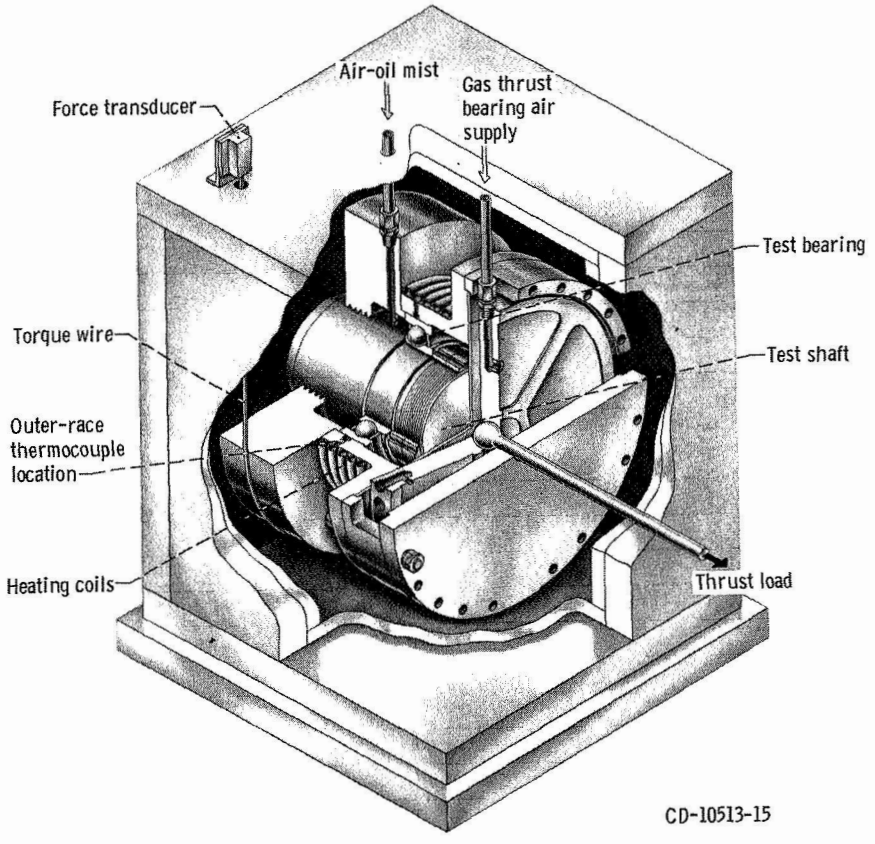

Figure 1. - Bearing test apparatus.

E-5442

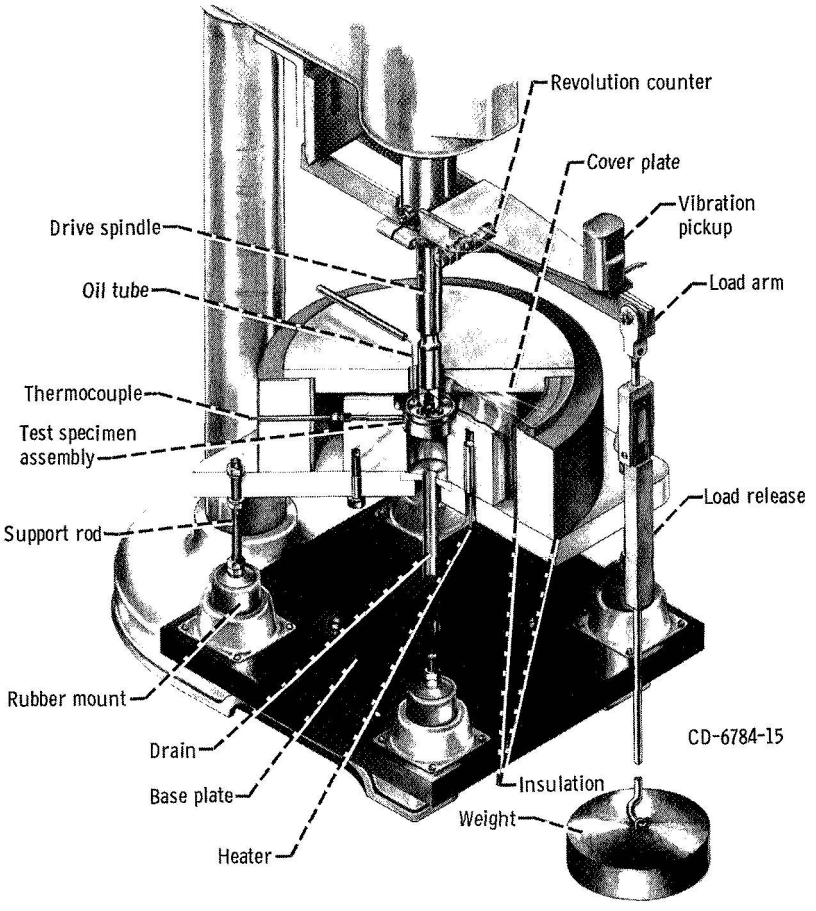

(a) Cutaway view of five-ball fatigue tester.

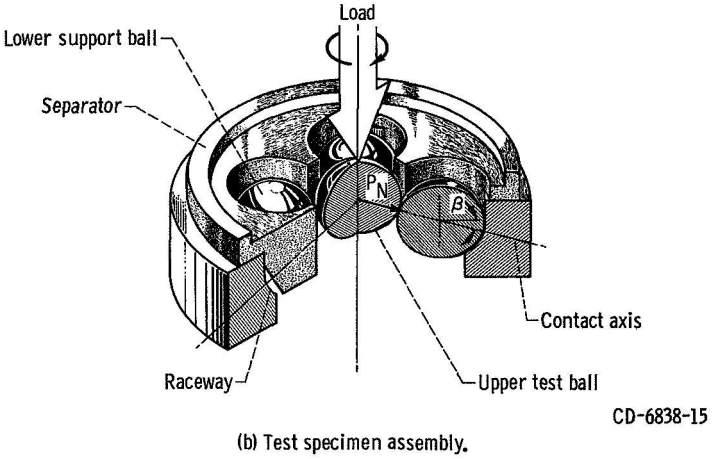

(b) Test specimen assembly.

Figure 2. - Five-ball fatigue tester.

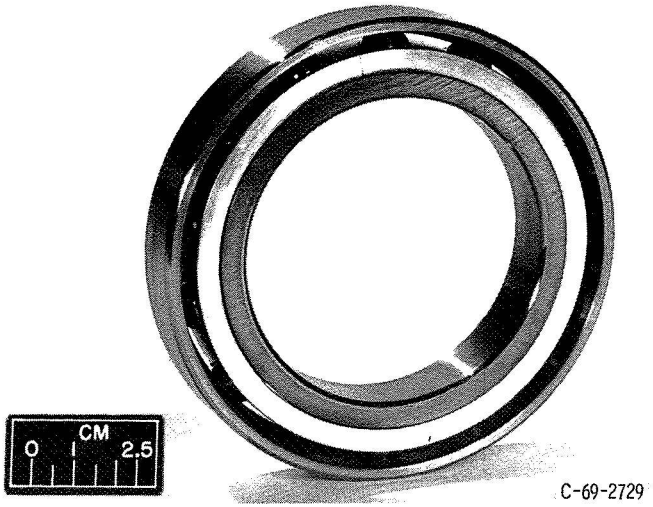

(a) Series 115: separable at outer race; one-piece cage construction; cage material, silver-plated iron-silicon-bronze.

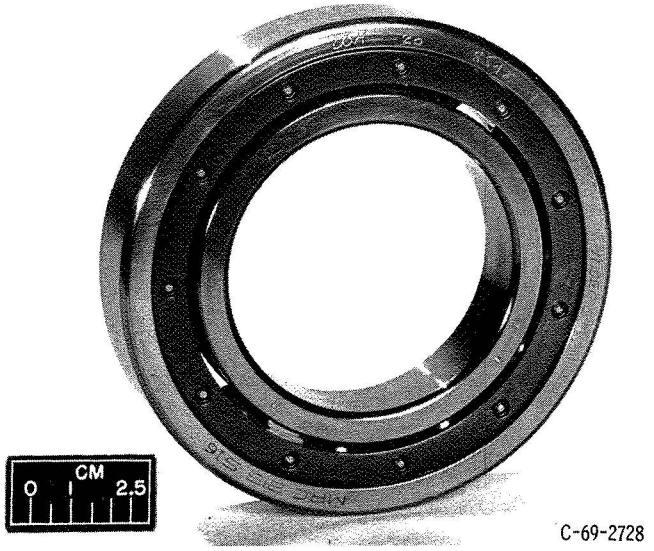

(b) Series 215: deep groove; two-piece machined cage construction; cage material, AISI M-2 tool steel.

Figure 3. - Test bearings.

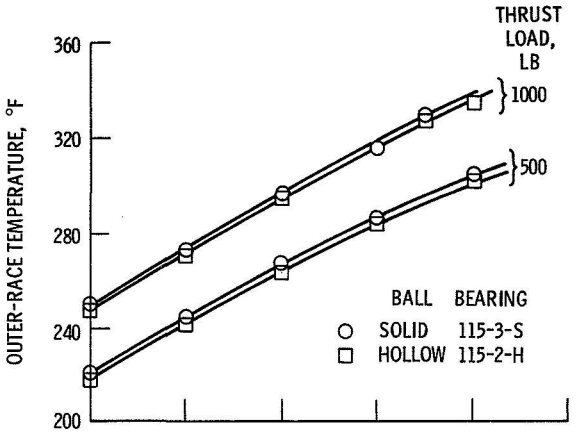

(a) Outer-race temperature as function of shaft speed.

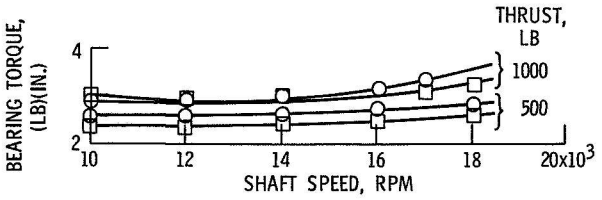

(b) Bearing torque as function of shaft speed.

Figure 4. - Comparison of performance data of series 115 75-millimeter bearings using both solid and hollow balls. Ball diameter, 1/2 inch (12.7 mm); ball material, SAE 52100 steel; bearing specifications given in table I.

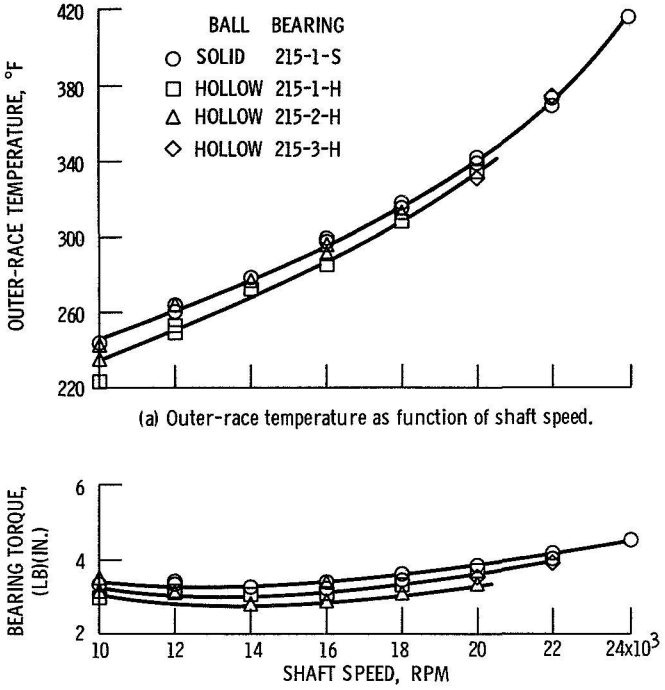

(a) Outer-race temperature as function of shaft speed.

(b) Bearing torque as function of shaft speed.

Figure 5. - Comparison of performance data of series 215 75-millimeter bearings using both solid and hollow balls. Ball diameter, 11/16 inch (17.5 mm); ball material, AISI M-2 for solid balls and AISI M-50 for hollow balls; thrust load, 500 pounds; bearing specifications given in table I.

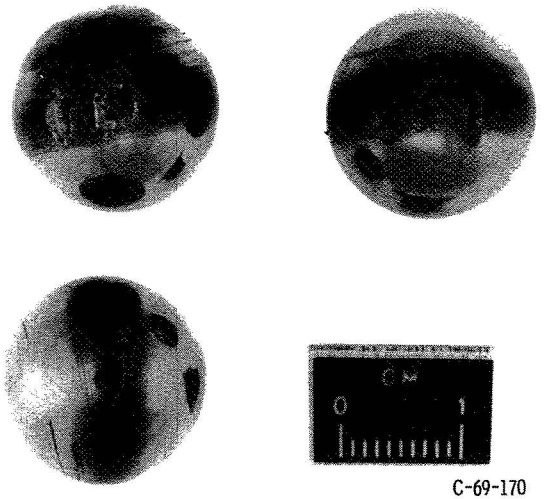

(a) Balls from bearing 215-1-H showing external spalls.

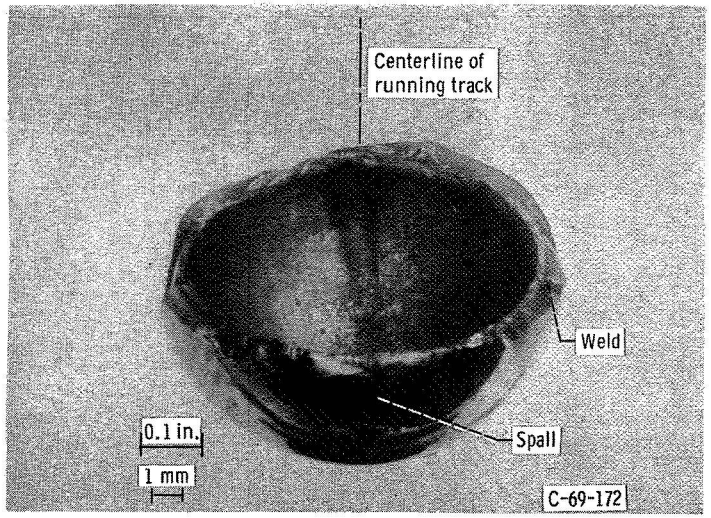

(b) Ball from bearing 215-3-H showing complete fracture.

Figure 6. - Typically damaged hollow balls from 215 series bearings.

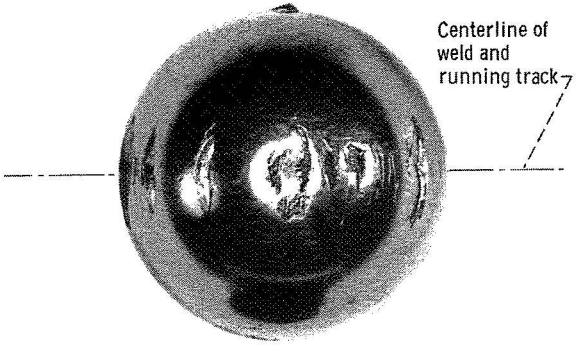

(a) View of external surface showing multiple spalls.

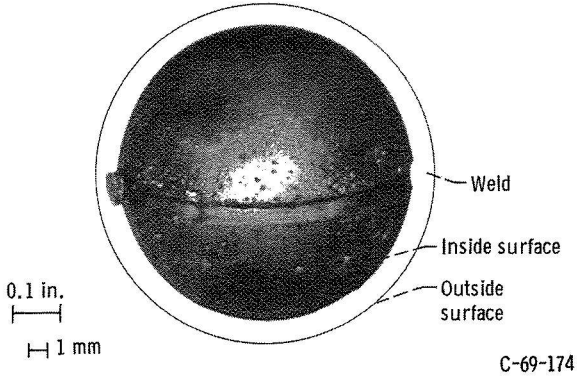

(b) View of internal surface showing weld.

Figure 7. - Ball from bearing 215-1-H with running track directly on weld area.

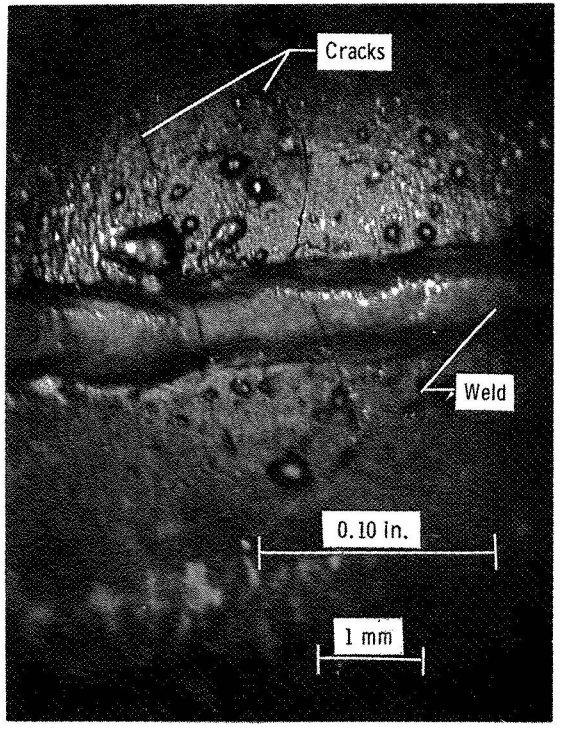

Figure 8. - Close-up view of weld bead of ball from figure 7(b) showing cracks on internal surface, across weld.

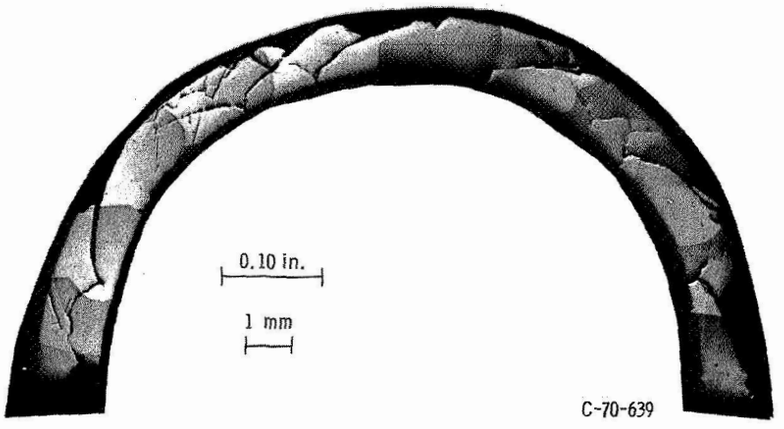

Figure 9. - Composite of photomicrographs of ball shown in figure 7 (from bearing 215-1-H) sectioned parallel to and through both the running track and the weld.

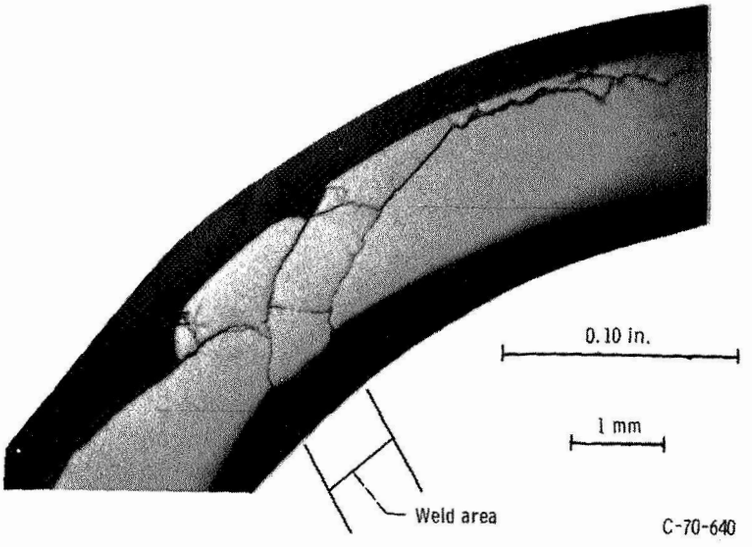

Figure 10. - Section view showing typical cracks between the weld area and the outside surface of the ball. Section taken parallel to and through the running track.

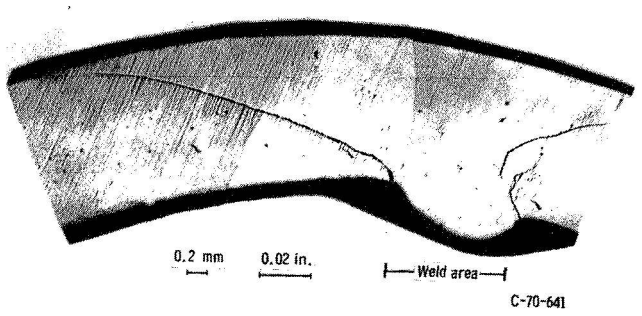

Figure 11. - Section of typical ball on which no surface spalls were evident, showing cracks originating at the weld area. Section taken parallel to and through running track. Ball from bearing 215-1-H.

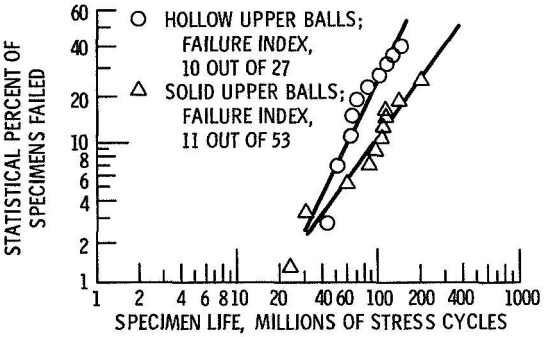

Figure 12. - Rolling-element fatigue life of SAE 52100 CVM steel hollow and solid balls in the five-ball fatigue tester. Maximum Hertz stress, 800,000 psi; speed, 10,600 rpm; no heat added; lubricant, super-refined naphthenic mineral oil.

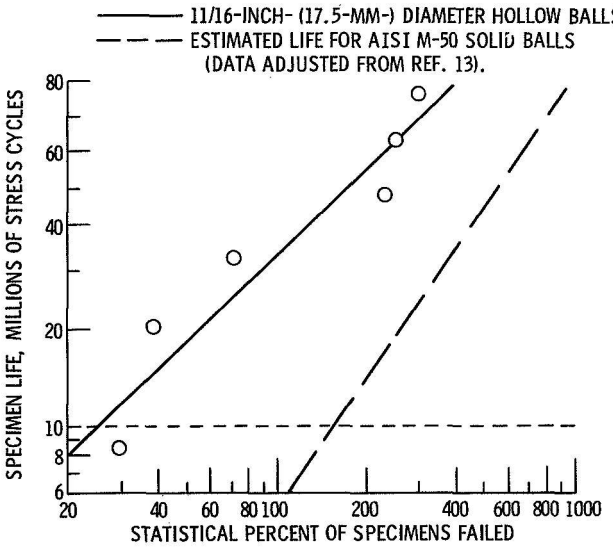

Figure 13. - Rolling-element fatigue life of AISI M-50 steel hollow and solid upper balls in five-ball fatigue tester. Maximum Hertz stress, 700 000 psi; speed, 10 600 rpm; lubricant, naphthenic mineral oil; no heat added.

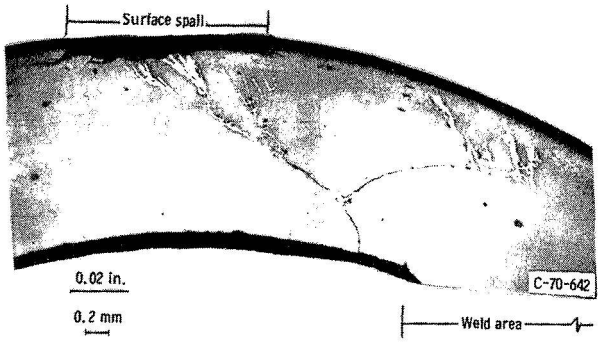

Figure 14. - Typical section through junction of weld and running track, showing crack connecting inside of wall with spall on outer surface. AISI M-50 steel, 11/16-inch (17.5 mm) diameter hollow ball; upper test ball in five-ball fatigue tester, 700 000 psi maximum Hertz stress. (Picral-HCL etch)